

ОБЪЕДИНЕННЫЙ
ИНСТИТУТ
ЯДЕРНЫХ
ИССЛЕДОВАНИЙ

Дубна

96-16

E14-96-16

V.Yu.Pomjakushin, A.A.Zakharov¹, A.Amato², V.N.Duginov,
F.N.Gygax², D.Herlach³, A.N.Ponomarev¹, A.Schenck²

STUDY OF MICROSCOPIC PHASE SEPARATION
IN $\text{La}_2\text{CuO}_{4+y}$ by μSR

Submitted to «Physica C»

¹RSC «Kurchatov Institute», Kurchatov sq.1, 123182 Moscow, Russia

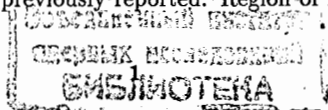
²Institut für Teilchenphysik der ETH Zürich, CH-5232 Villigen,
PSI, Switzerland

³Paul Scherrer Institut (PSI), CH-5232 Villigen, Switzerland

1996

1 Introduction

The problem of the coexistence of superconductivity (SC) and copper ion magnetism in HTSC was recognized just after the discovery of the copper oxide superconductors. In spite of a large number of experimental studies devoted to this topic, no conclusion on the form of such coexistence has yet been reached, i.e. whether SC and magnetic regions are space separated, and if so, what mechanism is responsible for this phase separation (PS). According to different theoretical approaches the electronic system possesses intrinsic tendency to a separation into regions with different electron (hole) concentrations [1-3]. This hypothesis has been successfully used to explain many experimental results [3-9]. Most of the experiments have been carried out on $\text{La}_{2-x}\text{Sr}_x\text{CuO}_{4+y}$ and provides only indirect evidences in favor of electronic PS. Certain hole concentration in this system can be achieved by various ways of doping. The equivalence of different (photo- or chemically) doping procedures of CuO_2 plane [10,11] in $\text{La}_2\text{CuO}_{4+y}$ has been experimentally verified. Furthermore, it has been found that photo-carriers are inhomogeneously distributed in the CuO_2 planes, forming metallic domains which are superconducting at low temperatures [10]. As far as the chemical doping of La_2CuO_4 is concerned it was shown that not only replacing of the trivalent La atoms by divalent Ba (or Sr), but also doping with extra oxygen generate a bulk superconductor with the same critical temperature of about 38K. Though the common properties of the both $\text{La}_{2-x}\text{Sr}_x\text{CuO}_{4+y}$ and $\text{La}_2\text{CuO}_{4+y}$ compounds are very similar, the "temperature-concentration" phase diagram differs drastically. It is believed that the difference is the result of different mobility of dopants. As a rule, extra oxygen atoms in $\text{La}_2\text{CuO}_{4+y}$ are considered as mobile impurities, that allows the system to be macroscopically phase separated. According to diffraction data a temperature reversible separation into two nearly identical orthorhombic phases takes place [12]. The oxygen rich ($y \simeq 0.06$) metallic phase becomes superconducting below $T_c = 38$ K, and a second insulating phase ($y \leq 0.01$) is antiferromagnetic (AFM). The phase domains of the oxygen rich regions have typical dimensions of about 3000 Å according to neutron diffraction data on the particle-size peak broadening [12]. From neutron diffraction measurements on polycrystalline electro-chemically oxidized $\text{La}_2\text{CuO}_{4+y}$ the miscibility gap limits were found to be $y = 0.01$ and $y = 0.06$ [13]. These boundaries are consistent with those found from NMR measurements on phase separated single crystals produced under high oxygen pressure [14]. The temperature of phase separation T_{ps} varies from 250 K to 415 K for the extra oxygen content inside the miscibility gap. High mobility of extra oxygen atoms being interstitial defects in crystalline lattice looks surprising at room temperatures. It is well known that oxygen mobility in ceramics is larger than in single crystals. In turn, oxygen diffusion in single crystals essentially depends upon its quality. It has been found that oxygen diffusion is very slow in $\text{La}_2\text{CuO}_{4+y}$ crystals grown at thermodynamically equilibrium conditions [15]. First, these crystals manifest themselves as a very good dielectric when extra oxygen is taken out of them by annealing. It allowed to assign a complete set of dipole-active IR modes [16] in IR spectra of La_2CuO_4 , because of the absence of the free carrier contribution. Then having been lightly doped with oxygen these crystals demonstrate quite different magnetic properties in comparison with those previously reported. Region of AFM phase ranges well



below the magic value $T_N = 250$ K – the Neel temperature in such crystals can be as low as $T_N \simeq 100$ K without any traces of PS and superconductivity [17,18]. It has been found [19] that at higher level of oxygen doping superconductivity appears but again in homogeneous system without magnetic order and PS. It is absolutely new modification of superconducting $\text{La}_2\text{CuO}_{4+y}$ where SC has been detected in *Bmab* crystallographic phase in system with immobile oxygen atoms. SC develops at a surprisingly low temperature $T_c = 12$ K lower than all previous finding. The non-PS crystal shows high sensitivity to the external magnetic field and a small Meissner fraction in contrast to PS crystal which demonstrates almost complete flux expulsion [19]. Despite this fact it is not a kind of weak superconductivity because the superconducting transition measured by resistivity survives in high magnetic fields up to 100 kOe. This result points to the absence of a direct relationship between SC and oxygen segregation in $\text{La}_2\text{CuO}_{4+y}$. In this respect it was very interesting to study the magnetic state of non-PS crystals $\text{La}_2\text{CuO}_{4+y}$ in more details. The μSR -technique, which is very sensitive to the local magnetic fields distributions, will provide a promising access to this problem.

μSR – muon spin relaxation, – is the experimental technique which allows one to observe time evolution of spin polarization of muons implanted into a sample. Polarized positive muons are stopped in the sample. After thermalisation, which takes negligible short time in comparison with the muon life-time $\tau = 2.2\mu\text{s}$, muon starts to rotate its spin around the local magnetic field. Then muon decays, emitting a positron preferably along its final spin direction. The spin precession or, more generally, the relaxation is detected as a time dependence of positron emission in a fixed direction. Histogram of time intervals between the moment of the muon stop in the sample and the moment of the registration of the positron in certain direction is μSR -spectrum. It has a form $N(t) = N_0 \exp(-t/\tau_\mu)(1 + P(t)) + N_{BG}$, where τ_μ is the muon lifetime, $P(t)$ is the time dependence of projection of the muon spin on the the given axis, containing muon spin interactions in the media. The hyperfine magnetic fields at the muon reflects local magnetic environment of the muon site. From the other hand the experimental μSR -signal is an average of the spin polarization of the muons distributed isotropically over the whole sample volume. Thus, the technique is a true bulk method of local magnetic fields measuring.

2 Samples. Experimental

The crystals of $\text{La}_2\text{CuO}_{4+y}$ were grown under equilibrium conditions by the molten solution method in which a single crystal holder was rotated under the surface of a molten solution [15]. Growth regime was used with 14.5 mol% of La_2O_3 and growth temperature $T_g = 1150$ K. As grown crystals showed Neel temperature $T_N = 270$ K. The crystal $\text{La}_2\text{CuO}_{4+y}$ was treated at $T=700$ C, $p=3$ kbar during 48 h, and then 24 h at $T=650$ C, $p=3$ kbar. The oxygen index $y = 0.03 \pm 0.005$ has been determined by weight gain, orthorombicity parameter and temperature of tetra-ortho transition. The crystal density is $\rho = 6.9$ g/cm³. The crystal revealed no traces of phase separation according to X-ray [19] (within temperature range $200 < T < 420$ K) and neutron diffraction [20] ($10 < T < 300$ K). The crystal becomes superconducting with $T_c = 12$ K measured

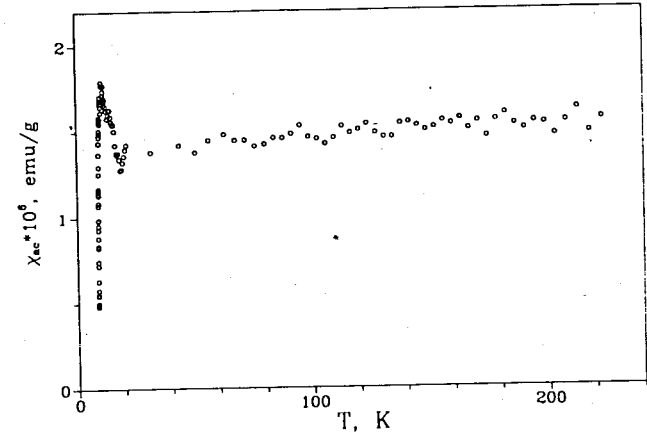


Figure 1: Magnetic susceptibility $\chi(T)$ for $H \parallel c$ in $\text{La}_2\text{CuO}_{4.03}$ crystal measured in alternating magnetic field with amplitude $H_0 = 0.8$ Oe, and frequency $F = 10$ kHz.

by dc-resistivity and magnetic susceptibility. Magnetoresistance has been measured on these crystals at high magnetic field up to 10 T [21]. Remarkable feature of the $T_c(H)$ dependence is the parallel shift of superconducting transition in magnetic field unlike the magnetoresistance in cuprates where fan-like behavior usually observed. The sharp onset of diamagnetism on $\chi(T)$ (Fig. 1) develops at 12 K. Diamagnetic response is very sensitive to the magnetic field – it is suppressed by external fields ~ 10 Oe. The results of magnetic susceptibility, X-ray and electrical resistivity measurements of the crystal were reported in [19] in details.

For μSR experiments the sample has been assembled of 3 pieces of the same single crystal. Total weight of the sample was about 80 mg. The pieces were glued to the silver plate mounted on the cold finger of the cryostat. The plate plane was mounted parallel to the muon beam with the sample glued in the way to cover the silver inside the beam spot. For changing the orientation of the crystal with respect to the external field it was remounted. The initial muon spin polarization was directed perpendicular to the c -axis of the crystal. Measurements have been made using GPS spectrometer on the πM3 surface muon beam line at PSI (Villigen).

3 Zero Field μSR -data

μSR -spectra has been taken for the initial muon spin polarization $P(0) \perp c$ at temperatures 3-100 K. Figure 2 shows the evolution of the polarization $P(t)$ with lowering temperature. Figure 3 shows initial time domain of the $P(t)$. In the temperature interval $T = 30 - 100$ K the time dependence of the muon spin polarization $P(t)$ has the

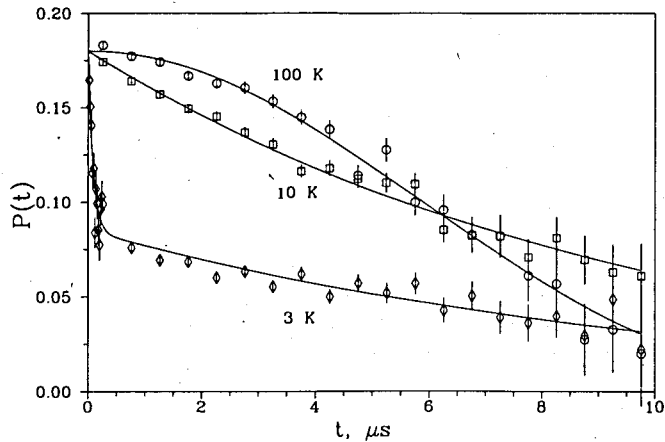


Figure 2: Time dependence of the muon spin polarization in zero external field in the $\text{La}_2\text{CuO}_{4.03}$ at the temperatures $T= 100$ K, 10 K, and 3 K.

static Kubo-Toyabe form:

$$G_{KT}(t) = 1/3 + 2/3 (1 - (\Delta t)^2) \exp(-(\Delta t)^2/2). \quad (1)$$

This fact provides the evidence of absence of the muon diffusion in the studied temperature interval. The relaxation rate has typical nuclear dipole value $\Delta = 0.14\mu\text{s}^{-1}$. In $\text{La}_2\text{CuO}_{4+y}$ nuclear dipole fields are produced by Cu^{63} , Cu^{65} and La^{139} nuclei. Particular value of the relaxation rate Δ depends on the muon site, crystal orientation with respect to initial muon spin polarization $P(0)$, and the direction of electric field gradient (EFG) on each nuclei. (we will discuss this subject in section 4).

Below 30 K the relaxation rate starts to increase, and the time dependence of the muon polarization becomes more exponential. Below the temperature $T_f = 8$ K the sharp increase of the muon spin depolarization occurs with relaxation rate achieving $12\mu\text{s}^{-1}$ at 3 K. The source of the increased depolarization is slowing down of the electronic magnetic moments fluctuations. In paramagnetic region ionic moments are fluctuating with large frequencies. Relaxation due to this mechanism is given by formula of extreme motional narrowing regime ($\nu_c \gg \omega_0$):

$$\lambda \sim \omega_0^2/\nu_c, \quad (2)$$

where $\omega_0 = \gamma_\mu B_{\mu,el}$ is a coupling constant determined by a typical magnetic field on the muon $B_{\mu,el}$ from electronic moments, ν_c is a fluctuation frequency. In paramagnetic region the main process contributing to ν_c is the exchange interaction between localized electronic moments $\nu_{ex} \simeq kT_N/\hbar \simeq 10^{11}T_N$ [Hz], where T_N is the magnetic ordering temperature in the system. ν_{ex} is temperature independent and larger than 10^{12} Hz for

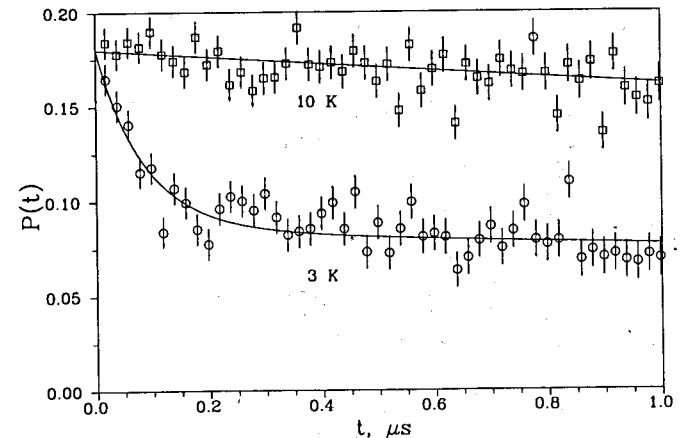


Figure 3: Initial part of time dependence of the muon spin polarization in zero external field in $\text{La}_2\text{CuO}_{4.03}$ at the temperatures 10 K, and 3 K.

the $\text{La}_2\text{CuO}_{4+y}$. Assuming that electronic fields are produced by Cu^{2+} ions, and taking the coupling constant $\omega_0 = 30\mu\text{s}^{-1}$ measured in AFM composition of La_2CuO_4 [22], the muon spin relaxation associated with this contribution is negligible $\lambda < 10^{-2}\mu\text{s}^{-1}$ in comparison with nuclear dipole relaxation. In the experiment this region of undetectable fast electronic fluctuations is roughly above 30 K. The slowing down of these fluctuations below 30 K increases the relaxation λ and owing to its dynamical origin changes the shape of the $P(t)$ to an exponential. One can see in fig. 2 that $P(t)$ at $T=10$ K has clear exponential shape. To describe the polarization $P(t)$ in the whole temperature region above T_f we use the phenomenological formula:

$$P(t) = A \exp(-\lambda t) G_{KT}(\Delta, t) \quad (3)$$

where λ is responsible for the fluctuations of the electronic moments, and Δ is the nuclear dipole relaxation. Figures 4 and 5 show temperature dependencies of the exponential λ and Gaussian Δ relaxation rates. Above 30 K the polarization is practically Gaussian with constant Δ . Below 30 K λ is increased without changing Δ down to ~ 10 K. Below 10 K the polarization converges to exponential shape with $\Delta = 0$, and $\lambda = 0.1\mu\text{s}^{-1}$. Gaussian relaxation can disappear if the electronic spins induce the nuclear spin relaxation. Let us estimate whether nuclear spins can relax at the given muon spin relaxation λ . Nuclear relaxation in motional narrowing limit is:

$$\nu_N = (\gamma_N B_{hf})^2/\nu_{el}, \quad (4)$$

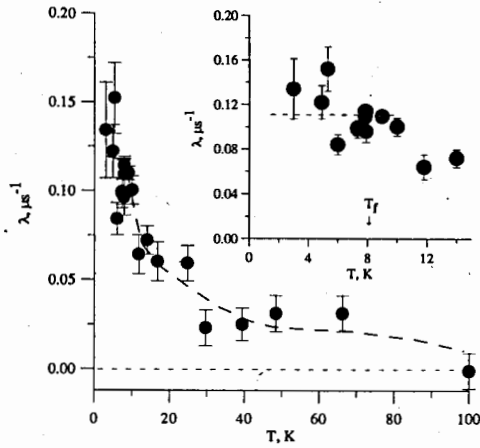


Figure 4: Exponential relaxation of polarization in $\text{La}_2\text{CuO}_{4.03}$ in zero external field. Polarization was fitted to (3). Below $T_f = 8$ K the relaxation rate λ_s of slow damping component is given. Insert shows low temperature domain.

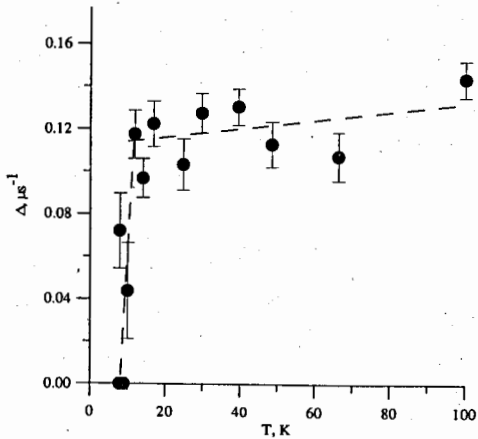


Figure 5: Gaussian relaxation Δ of polarization fitted to (3) in $\text{La}_2\text{CuO}_{4.03}$ in zero external field.

where B_{hf} is the hyperfine magnetic field on the nuclei, ν_{el} is the fluctuation frequency of the electronic spins. Comparing ν_N with λ one finds that $\nu_N = (\gamma_N/\gamma_\mu)^2 (B_{\text{hf}}/B_{\mu,el})^2 \lambda$. Fluctuations of nuclear spins can narrow the Gaussian relaxation only if $\nu_N > \Delta$. Taking $\lambda = 0.1 \mu\text{s}^{-1}$, $\gamma_N/\gamma_\mu \sim 0.3$, and the nuclear dipole width $\Delta = 0.1 \mu\text{s}^{-1}$ one obtains $B_{\text{hf}}/B_{\mu,el} > 3$. This is quite reasonable for copper nuclei since the magnetic field B_{hf} produced by Cu^{2+} -spin on its nuclei is significantly greater than the magnetic field on the remote muon. Thus, nuclear dipoles can relax in our case, and decrease in Δ reflects this process.

Below $T_f = 8$ K the polarization splits up into two components: one is fast damping with relaxation rate λ_f , and the second one has slow relaxation rate λ_s . The both components are well fitted to exponential relaxation functions. Total polarization reads:

$$P(t) = A_f \exp(-\lambda_f t) + A_s \exp(-\lambda_s t) \quad (5)$$

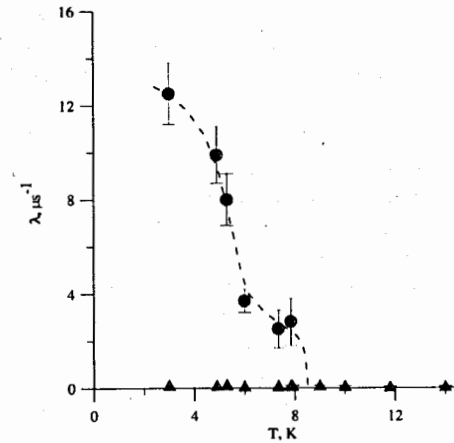


Figure 6: Relaxation rate of the fast (λ_f , circles) and slow (λ_s , triangles) damped component of polarization in $\text{La}_2\text{CuO}_{4.03}$ in zero external field. Points above $T_f = 8$ K is the relaxation rate of one component signal.

Figure 6 shows the fast relaxation rate λ_f as a function of temperature. λ_s is shown in the insert of of the Fig. 4. Figure 7 depicts temperature dependencies of asymmetries. Asymmetries A_f and A_s divided by the total experimental asymmetry $A_0 = 0.18$ represent volume fractions of the crystal which possess significantly different magnetic environment for the muon spin. Above T_f the crystal is homogeneous for the muon and the signal is one-component with full asymmetry A_0 , as shown in fig. 7. Below T_f in the part of the crystal the muon spin is strongly depolarized due to interactions with frozen electronic spins. This fraction steadily increases with decreasing the temperature reaching half of the total signal at 3 K. The electronic spins in "frozen" part

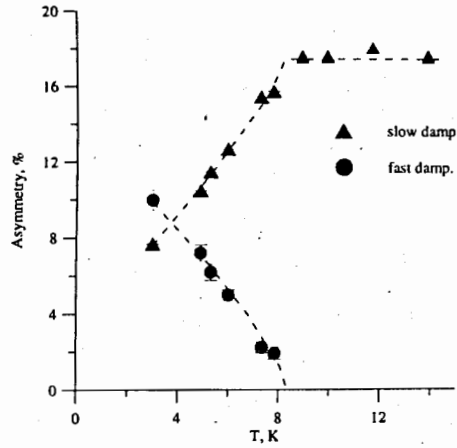


Figure 7: Asymmetries of the two-component signal below T_f in $\text{La}_2\text{CuO}_{4.03}$ in zero external field as functions of temperature. Triangles show asymmetry of the slow damping paramagnetic fraction, circles show asymmetry of the fast damping magnetic fraction.

of the crystal are not completely static. This follows from the time dependence of $P(t)$ (see Fig. 3), that does not have minimum at a time point $t \sim \Delta^{-1}$ typical for any static magnetic field distribution with the r.m.s. average magnetic field on the muon Δ/γ_μ . However, the value of the relaxation rate $\lambda_f(3\text{K}) = 12\mu\text{s}^{-1}$ is relatively large pointing that field distribution is close to static limit. This relaxation rate corresponds to the local field $B_\mu = 140$ G assuming that it is static. The value has same order of magnitude as those in antiferromagnetic $\text{La}_2\text{CuO}_{4+y}$ samples $B_\mu = 400$ G, and in spin-glass ordered $\text{La}_{2-x}\text{Sr}_x\text{CuO}_{4+y}$ $B_\mu = 200$ G [22]. To estimate the fluctuation frequency one has to choose appropriate magnetic field on the muon. Tentatively taking 200-400 G the fluctuation frequency of the electronic moments at $T=3$ K amounts $10^7 - 10^8$ Hz.

The slow relaxing component has exponential shape (Gaussian relaxation function gives worse χ^2 -criteria), and its relaxation rate λ_s , is not practically changed below the transition temperature (fig. 4). This fact evidences that the electronic moment fluctuations have been also slowed down in the paramagnetic parts of the crystal. Paramagnetic fraction decreases with lowering temperature (fig. 7) implying that the "frozen" part of the crystal grows by means of gradual transition of paramagnetic parts of the crystal to "frozen" state. Actually, such a behaviour suggests idea that crystal undergoes wide temperature transition to spin frozen state as a whole.

We have to note that two-component-like form of polarization can be also fitted to stretched exponential time dependence of muon spin polarization:

$$P(t) = A \exp(-(\lambda t)^\alpha). \quad (6)$$

This $P(t)$ is actually an empirical type law. There are few values of the exponent α which correspond to physical cases with known meaning of the parameters contained in stretched exponential law (6). When the exponent α is equal to unity formula (6) gives just exponential shape of $P(t)$ corresponding to standard motional narrowing regime in the limit of fast fluctuations. Root exponential dependence ($\alpha = 1/2$) is provided by dilute spin glasses formalism [24] and indeed was experimentally observed.

Fits of experimental data with formula (6) gives a bit worse χ^2 in comparison with two-component description of time polarization (5), but χ^2 still get into one confidence interval of χ^2 -distribution, except of one experimental point at $T = 3$ K. Hence, we have to discuss a possibility of such $P(t)$ description as well. Figure 8 shows parameters of stretched exponential polarization function: the relaxation rate λ , and the exponent α as functions of temperature. The exponent α is monotonically decreased from $\alpha = 1$ at the temperatures just above the transition temperature $T_f = 8$ K down to $\alpha \simeq 0.3$ at the lowest measured temperatures. Physical meaning of this "1/3" exponent values and the corresponding relaxation rates is not clear (i.e. it is hardly possible to associate them with parameters of internal fields distribution, such as their magnitudes and fluctuation frequencies). Nevertheless, such values of exponent have been experimentally detected in different spin-glass systems at the temperatures near the magnetic transition, for example in the canonical spin-glasses AuMn [25]. This $P(t)$ shape was interpreted in terms of the distribution of the electronic spin correlation times. Fast initial depolarization, which becomes more pronounced when approaching T_f , reflects an increase in the weight of low frequency part of the spectral distribution of correlation times. However, interpretation of the present data in terms of two exponential polarization function looks more relevant because this simplest

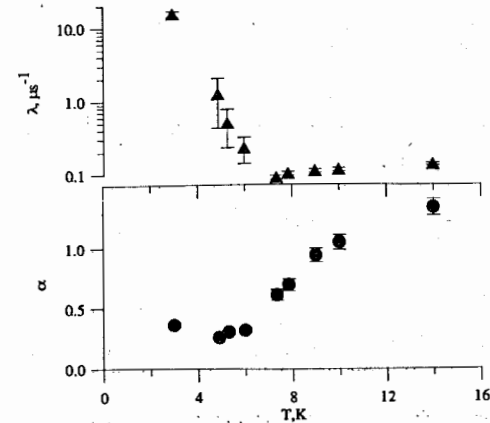


Figure 8: Relaxation rate λ (upper part), and power coefficient α (bottom part) of the ZF polarization function fitted to formula (6).

and reasonable assumption of spatially separated regions with considerably different fluctuation frequencies provides best χ^2 , clear meaning of the polarization components, and nice sensible temperature dependencies of asymmetries.

4 Muon site

The $(1/2, 1/2, 1/4)$ part of the La_2CuO_4 unit cell is shown in the Fig. 9. We use tetragonal notation of the axes. Lattice constants $a = b = 3.779 \text{ \AA}$, $c = 13.2 \text{ \AA}$. It is reasonable to assume that muon site is situated close to oxygen - the only negative ion in the system. Theoretical cluster calculations [26] gives the absolute Coulomb potential minimum for the muon in the point in the (ac) plane $R_{\mu, \text{theor}} = (0.12, 0, 0.11)$, which is 1.08 \AA apart from apical oxygen O2. The local magnetic field 430 G on the muon observed in antiferromagnetic $\text{La}_2\text{CuO}_{4+y}$ limits the muon site to the positions which are relatively far from Cu^{2+} ions. The muon site deduced from the dipole field calculation (assuming point dipoles Cu^{2+}) [23] is situated in the (ac) plane at the distance of 1 \AA from oxygen: $R_{\mu, \text{Hitti}} = (0.253, 0, 0.162)$. Actually, the hyperfine field on the muon can have a significant (about 50%) local dipolar field contribution in addition to point dipole one [26]. This is also supported by the experiment on the single crystal of AFM $\text{La}_2\text{CuO}_{4+y}$, where authors determined the direction of the local field on the muon [27]. In point dipole calculation the local field could not be reproduced for any point in the crystal, except unique site unphysically close to planar oxygen. Thus, in spite of good correspondence of B_μ for $R_{\mu, \text{Hitti}}$ with the experimental one,

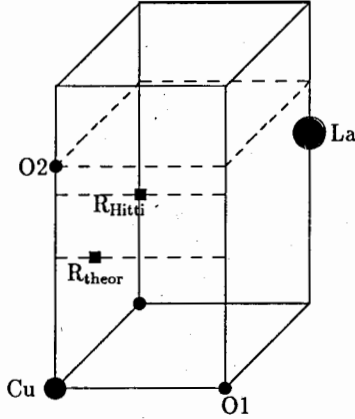


Figure 9: $(1/2, 1/2, 1/4)$ of the La_2CuO_4 unit cell. Squares show the muon sites proposed by [23] - $R_{\mu, \text{Hitti}} = (0.253, 0, 0.162)$, and $R_{\mu, \text{theor}} = (0.12, 0, 0.11)$ - [26]. Both sites are on the (ac) plane.

some uncertainty in the muon site is present because of local dipole contribution.

Another bit of information on the muon site comes from the nuclear dipole relaxation in ZF experiment. In $\text{La}_2\text{CuO}_{4+y}$ nuclear dipole fields are produced by Cu^{63} , Cu^{65} and La^{139} nuclei. Oxygen nuclei do not possess magnetic moments. Experimentally, the nuclear dipolar width can be measured at low temperatures in paramagnetic state of the samples $\text{La}_{2-x}\text{Sr}_x\text{CuO}_{4+y}$ which are superconducting or magnetic with low transition temperature. In polycrystalline SC $\text{La}_{1.85}\text{Sr}_{0.15}\text{CuO}_{4+y}$ [23] and SG $\text{La}_{1.93}\text{Sr}_{0.07}\text{CuO}_{4+y}$ [28] dipolar width is $\Delta = 0.17 \mu\text{s}^{-1}$. This value agrees perfectly with the calculated width for the muon site $R_{\mu, \text{Hitti}}$ in assumption that that EFG is along muon-nuclei direction (REFG). In present experiment with the single crystal of $\text{La}_2\text{CuO}_{4.03}$ the dipolar width for $P(0) \perp c$ is $\Delta = 0.14 \mu\text{s}^{-1}$. The crystal consisted of two twin orientations in the (ab) plane, and orientation of $P(0)$ within (ab) plane was not known. Calculated values of Δ at muon site $R_{\mu, \text{Hitti}}$ for REFG with $P(0)$ directed along a and b axes are: $\Delta_a^{\text{rad}} = 0.184 \mu\text{s}^{-1}$, $\Delta_b^{\text{rad}} = 0.145 \mu\text{s}^{-1}$. For the EFG along c axis (this direction has been reported in NQR papers [29]) the dipole widths are smaller: $\Delta_a^{\text{ax}} = 0.138 \mu\text{s}^{-1}$, $\Delta_b^{\text{ax}} = 0.132 \mu\text{s}^{-1}$. Taking into account that actual EFG direction is some average of muon induced REFG and natural EFG we conclude that $R_{\mu, \text{Hitti}}$ do not contradict our ZF data. Muon site $R_{\mu, \text{theor}}$ proposed from Coulomb energy calculations is unfavorable since dipolar widths for this site are too large in comparison with experiment: $\Delta_a^{\text{ax}} \simeq \Delta_b^{\text{ax}} = 0.29 \mu\text{s}^{-1}$, $\Delta_a^{\text{rad}} = 0.319 \mu\text{s}^{-1}$, $\Delta_b^{\text{rad}} = 0.325 \mu\text{s}^{-1}$. Further, in the Knight shift calculations we use the most appropriate to our data muon site $R_{\mu, \text{Hitti}}$.

5 Transverse Field experiment

5.1 Contributions to the magnetic field on the muon

The effective magnetic field at the muon site is given by:

$$\vec{B}_\mu = \vec{H}_{\text{ext}} + \vec{B}_{\text{dip}} + \vec{B}_L + \vec{B}_c \quad (7)$$

where \vec{B}_{dip} is the dipolar field from neighbor magnetized ions, \vec{B}_L is Lorentz and demagnetization fields, and \vec{B}_c is the contact hyperfine field. The direction of $\Delta\vec{B}_\mu = \vec{B}_\mu - \vec{H}_{\text{ext}}$ do not coincide with \vec{H}_{ext} , but since $\Delta B_\mu \ll H_{\text{ext}}$ only the projection $(\Delta\vec{B}_\mu \cdot \vec{H}_{\text{ext}})/H_{\text{ext}}$ contributes to the total field B_μ , which is experimentally measured.

Knight shift of the B_μ reads:

$$K_\mu = (\Delta\vec{B}_\mu \cdot \vec{H}_{\text{ext}})/H_{\text{ext}}^2 \quad (8)$$

In the paramagnetic state the magnetic moment $\vec{\mu}_i$ of the given sort of ions i is induced by the external magnetic field, and the value of the moment is given by the atomic susceptibility χ_{at} as $\mu = H_{\text{ext}}\chi_{at}$. The point magnetic dipoles produce the dipolar field \vec{B}_{dip} :

$$\vec{B}_{\text{dip}} = \sum_i \hat{A}_{\text{dip}}(i) \vec{\mu}(i) \quad (9)$$

Dipolar tensor $\hat{A}_{dip}(i)$ is determined by particular muon site and the sublattice i of the magnetic atoms.

$$\hat{A}_{dip}(i) = \sum_{\vec{r}(i)} \frac{1}{r^3} \left(\frac{3r_\alpha r_\beta}{r^2} - \delta_{\alpha\beta} \right), \quad (10)$$

where sum is performed over all ions in i -th sublattice inside the Lorentz sphere, $\vec{r}(i)$ are the distances between the muon and the ions. When H_{ext} is parallel to the α -axis the corresponding Knight shift reads:

$$K_{dip,\alpha}(i) = A_{dip,\alpha\alpha}(i) \chi_{\alpha\alpha}(i) \quad (11)$$

The contact field on the muon \vec{B}_c is also proportional and parallel to the external field. The contact contribution to K_μ is given by the coupling constant A_c . There are several sources of A_c . First one is the spin density on the muon due to the unpaired spin orbitals. The second one is the indirect RKKY interaction producing an additional spin polarization of the conduction electrons. Both of them are proportional to the atomic susceptibility. And the last contribution comes from Pauli paramagnetism of the conduction electrons, which is temperature independent.

Lorentz and demagnetization fields are proportional to the volume magnetic susceptibility χ . Demagnetization field averaged over sample is parallel to the external field. Their contribution to the Knight shift is:

$$K_L = (4\pi/3 - N)\chi, \quad (12)$$

where N is the demagnetization factor of the sample.

Total Knight shift on the muon reads:

$$K_\mu = K_{dip} + K_L + A_c \quad (13)$$

5.2 Knight shift data

Transverse field experiment (TF) has been performed with two sample orientations: H_{ext} is parallel and perpendicular to the tetragonal c -axis of the crystal.

Figure 10 shows temperature dependence of the muon precession frequency for both orientations of the crystal in the external field $H_{ext} = 2$ kOe, right y-axis represents the corresponding Knight shift value. The absolute value of the external field has been measured by NMR probe in the place of the sample only for $H_{ext} \parallel c$ orientation. For the second orientation the current in the Helmholtz coils which produce magnetic field was set to approximately same value, but the external field in the sample place has not been measured with NMR probe, and due to that some systematic shift of H_{ext} could be present for $H \perp c$. Temperature dependence of the magnetic susceptibility $\chi(T)$ (Fig. 1) reveals very slight slope in the interval 20-250 K. An increase in χ below 20 K is probably connected with the Curie-Weiss contribution due to spin freezing transition at $T_f = 8$ K. The sharp χ decreasing below 12 K occurs when the crystal enters the superconducting state. $K_\mu(T)$ reveals significantly more strong temperature dependence, which obviously does not scale with the susceptibility. It starts to decrease

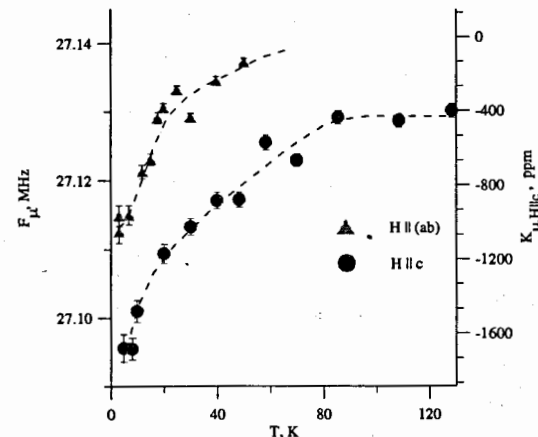


Figure 10: Muon precession frequency as a function of temperature in $\text{La}_2\text{CuO}_{4.03}$ for $H \parallel c$ and $H \perp c$, $H_{ext} = 2$ kOe. Right y-axis represents corresponding Knight shift value for $H \parallel c$ orientation.

already below $T=80$ K, which is larger than any reasonable superconducting transition in this system.

Main expected contribution to the Knight shift K_μ is dipolar fields from Cu^{2+} magnetic moments. Dipolar tensor of Cu^{2+} sublattice for the muon site $R_{\mu,H||c}$ in the basis of the tetragonal axes reads:

$$\hat{A}_{dip}(\text{Cu}^{2+}) = \begin{pmatrix} -0.362 & 0 & 0.578 \\ 0 & -0.805 & 0 \\ 0.578 & 0 & 1.167 \end{pmatrix} \begin{bmatrix} \text{kG} \\ \mu_B \end{bmatrix}. \quad (14)$$

Assuming that only Cu^{2+} ions contributes to the susceptibility the Knight shift along α -axis reads:

$$K_{dip,\alpha} = A_{dip,\alpha\alpha}(\text{Cu}^{2+}) [G/\mu_B] \chi_{mol,\alpha} / (N_A \mu_B). \quad (15)$$

Where N_A is Avogadro number, μ_B is Bohr magneton. The molar susceptibility of the $\text{La}_2\text{CuO}_{4.03}$ crystal along c -axis is $\chi_{mol,c} = 5 \cdot 10^{-4}$ emu/mol. According to (14) $K_{dip,c} = +100$ ppm. It has wrong sign, and at least 4 times less than experimental K_μ . It is quite possible that proposed muon site is not correct, but to get the right order of magnitude one has to put the muon closer to the Cu^{2+} ions. This is, actually, hardly possible since we would get in this case proportionally increased local field on the muon in AFM ordered samples $\text{La}_2\text{CuO}_{4+y}$, and also significantly increased ZF nuclear dipole width.

Lorentz contribution K_L according to (12) is in the range from -60 ppm to 30 ppm for the demagnetization factor N from 0 to 4π .

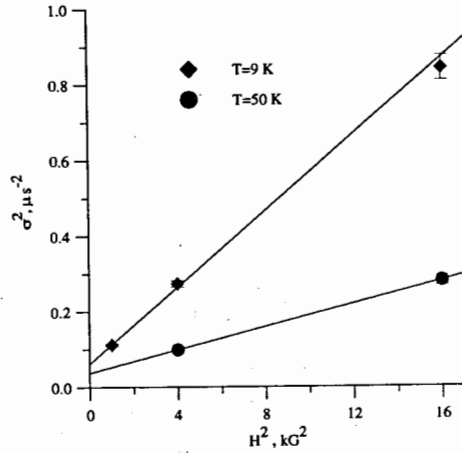


Figure 11: Square of Gaussian relaxation rate σ^2 as a function of external field in $\text{La}_2\text{CuO}_{4.03}$ at 50 K and 9 K.

All these contributions are small and can not provide experimental $K_\mu(T)$ dependence. To get an agreement with the absolute Knight shift values one has to assume that there is either large RKKI contact contribution to the K_μ produced by Cu^{2+} , or contribution from closest to muon oxygen ion. Taking the $\mu^+ - \text{O}$ distance $\sim 1 \text{ \AA}$ one gets the dipolar tensor components of the order $10 \text{ kG}/\mu_B$, which are large enough.

5.3 Field induced broadening of K_μ distribution

The muon spin polarization has been fitted to the Gaussian relaxing function:

$$P(t) = A \exp(-(\sigma t)^2/2) \cos(2\pi f t + \varphi) \quad (16)$$

Where σ is the relaxation rate, f - muon precession frequency. To clarify the source of the relaxation σ , external field scans at $T=50 \text{ K}$ (far paramagnetic region where both K_μ and σ are on a plateau) and 9 K (below $T_c = 12 \text{ K}$, but above $T_f = 8 \text{ K}$) have been performed for $H_{\text{ext}} \parallel c$. Figure 11 shows field dependence of the Gaussian relaxation rate σ in the axes $\sigma^2(H^2)$. In the single crystalline sample far above T_f main expected source of the muon spin relaxation is nuclear dipole fields. This broadening is not scaled with the external field. It is surprising that in our case the relaxation rate σ has a large contribution which scales with the external field. This behaviour would be quite normal for polycrystalline samples, where it is originated from angular dependence of the K_{dip} , but is absolutely not expected for the single crystal. There are two contributions to σ :

$$\sigma^2 = \sigma_n^2 + \sigma_b^2, \quad (17)$$

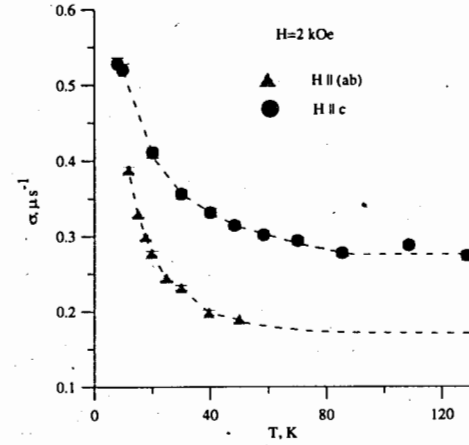


Figure 12: Gaussian relaxation rate as a function of temperature in $\text{La}_2\text{CuO}_{4.03}$ for $H \parallel c$ and $H \perp c$.

where σ_n is nuclear dipole value, $\sigma_b = \gamma_\mu H_{\text{ext}} k_\sigma$ is an additional broadening which scales with H_{ext} . k_σ is the half-width of the field distribution normalized by the $\omega_{\text{ext}} = \gamma_\mu H_{\text{ext}}$. By fitting the data to (17) one obtains $\sigma_n = 0.194 \pm 0.015 \mu\text{s}^{-1}$, $k_\sigma = 1450 \pm 50 \text{ ppm}$ for $T=50 \text{ K}$, and $\sigma_n = 0.249 \pm 0.008 \mu\text{s}^{-1}$, $k_\sigma = 2640 \pm 50 \text{ ppm}$ for $T=9 \text{ K}$. Increased value of σ_n at 9 K reflects contribution from dynamical fluctuations of electronic moments, which is also independent of H_{ext} .

Below 30 K the field distribution is becoming more like Lorentzian. In comparison with the Gaussian shape it has more wider tails around the peak. This kind of distribution gives $P(t)$ which can be fitted to both damped Gaussian (function (16) multiplied by $\exp(-\lambda t)$) and two Gaussian $P(t)$. Since the physics behind these distributions is not clear for a moment we will describe the damping of the $P(t)$ by an averaged σ from one Gaussian fit (16). Actually, the χ^2 -criteria for this description remains quite good at the temperatures above T_f .

The relaxation rate σ is plotted as a function of temperature in Fig. 12. The increase in relaxation rate scales with the increase in the absolute value of the Knight shift (compare figures 10 and 12). Note, that there is no peculiarity in $\sigma(T)$ in the temperature of superconducting transition $T_c = 12 \text{ K}$, implying that no Abrikosov flux line lattice is formed in the crystal volume. Figure 13 shows the reduced broadening $k_\sigma = \sigma_b/\omega_{\text{ext}}$ as a function of the Knight shift K_μ for $H_{\text{ext}} \parallel c$ direction. Field induced broadening σ_b was calculated from experimental values of σ by subtracting nuclear dipole relaxation value $\sigma_n = 0.194 \pm 0.015 \mu\text{s}^{-1}$ according to the formula (17). The $k_\sigma(K_\mu)$ is near linear for temperatures $T > 30 \text{ K}$ (small $|K_\mu| \leq 1000 \text{ ppm}$). Strong nonlinear increase in k_σ at large $|K_\mu|$ (corresponding to the temperatures below $\sim 30 \text{ K}$) is caused by the slowing down of the electronic spins fluctuations, which is revealed in

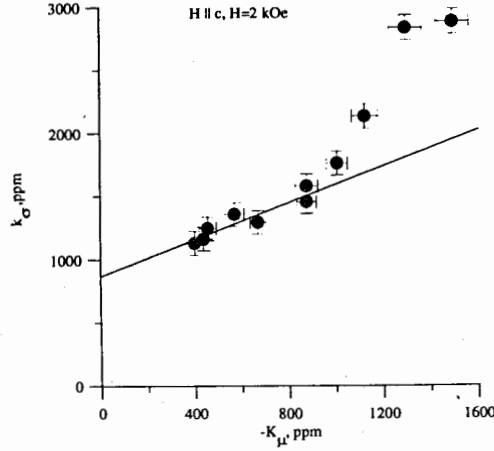


Figure 13: Reduced field induced broadening k_σ is shown as a function of the Knight shift K_μ for $H_{\text{ext}} \parallel c$ for the temperatures 5-130 K

the ZF-field data, as well. Fitting the initial part of $\sigma_b(K_\mu)$ dependence one obtains the following linear relation between reduced broadening k_σ and Knight shift K_μ :

$$k_\sigma = -k_{\sigma/K} K_\mu + k_{\sigma 0}, \quad (18)$$

where $k_{\sigma/K} = 0.72 \pm 0.19$, $k_{\sigma 0} = 868 \pm 12$ ppm.

5.4 Sources of the field induced broadening σ_b

Existence of the field induced broadening in the single crystal immediately leads us to the conclusion that the local magnetic environment of the muon is changed over the sample volume. The idea that the phase separation on the microscopic scales exists in the $\text{La}_2\text{CuO}_{4.03}$ crystal will provide only small part of line broadening.

Let us suppose that the sample is separated in the manner similar to the samples which demonstrate macroscopic phase separation into the oxygen rich $y \simeq 0.06$ and oxygen poor $y \simeq 0.01$ domains. The domain sizes are small (at least $< 10^3 \text{ \AA}$), because no traces of any phase separation have been found by X-ray and neutron diffraction. Since the stoichiometry of the oxygen in our sample is $y \simeq 0.03$ the volumes of both fractions are approximately equal. For convenience we will denote oxygen rich fraction as *SC* (Superconducting, metallic), and oxygen poor one as *M* (Magnetic, isolating).

First, we should note that when the SC-fraction goes to the superconducting state the external magnetic fields does not form a vortex lattice. Even single vortex line can not fit into the small domain, because the London penetration depth λ is larger than 2000 \AA in this system. The magnetic field decays exponentially into the SC-domain as in a type-I superconductor:

$$B(x) \sim \left(H_{\text{ext}} / \cosh\left(\frac{\delta}{2\lambda}\right) \right) \cosh\left(\frac{x}{\lambda}\right), \quad (19)$$

where x -axis origin is in the centre of the domain. The field inhomogeneity and average induction in the domain read:

$$\Delta B \sim \frac{1}{2}(H_{\text{ext}} - B(0)) \sim H_{\text{ext}} \frac{1}{16} \left(\frac{\delta}{\lambda}\right)^2, \quad (20)$$

$$\langle B \rangle \sim H_{\text{ext}} - \Delta B$$

where δ is the domain size. One can see that the field variance is scaled with the external field and can be small for small domains δ in opposite to the flux lattice case where it is field independent and determined only by London penetration depth λ . This contribution, of course, can not be revealed above T_c which is not expected to be larger than 40 K. Experimentally we see an increase in σ and a decrease K_μ already below 80 K.

Second, consider the contribution due to the difference in the susceptibility χ of SC- and M-domains above any transitions (magnetic and superconducting). Knight shift is determined by effective coupling constant A_{eff} . Assuming the same coupling constant in both domains variance of Knight shift $\Delta K_\mu = A_{\text{eff}}(\chi_{\text{SC}} - \chi_{\text{M}})$ can give reduced broadening $k_\sigma = \Delta K_\mu / 2$, which will never be larger than average $\langle K_\mu \rangle$ value even for $\chi_{\text{M}} / \chi_{\text{SC}} = 0$. In the experiment the ratio k_σ / K_μ is significantly greater (see fig. 13).

Third, Lorentz and demagnetization fields give contribution to the field variance proportional to the volume susceptibility which can not exceed:

$$\Delta B_L = H_{\text{ext}} 4\pi(\chi_{\text{SC}} - \chi_{\text{M}}) / 2 \quad (21)$$

Susceptibility above T_c is $\chi = 7 \cdot 10^{-6} \text{ emu/cm}^3$, so this contribution is negligible: $k_\sigma = \Delta B_L / H_{\text{ext}} \sim 40$ ppm.

Considered contributions to the field induced broadening are caused by presence of mixture of two phases with different macroscopic magnetic properties. These contributions are small and can not account for experimental broadening k_σ . The broadening k_σ exceeds the Knight shift K_μ , as follows from the formula (18). The Knight shift spread exceeds the average K_μ at least 2 times. Extrapolating $k_\sigma(K_\mu)$ to $K_\mu = 0$ gives the broadening $k_{\sigma 0} \simeq 870$ ppm. Actually, we can extrapolate to $K_\mu \simeq +100$ ppm corresponding to the expected Knight shift value from Cu^{2+} sublattice. However, it does not significantly change $k_{\sigma 0}$ value. Large constant term $k_{\sigma 0}$ in $k_\sigma(K_\mu)$ dependence implies that the distribution of the Knight shift contains both positive and negative K_μ . Assumption of just a variance in the atomic susceptibility is not enough to describe such a distribution because in this case $k_{\sigma 0}$ has to be zero. To get such wide Knight shift distribution one has to suppose that there is a distribution of effective coupling constants. This situation can be modeled with help of an "impurity" (e.g. the extra oxygen ions or micro-regions of atomic scales) which possesses large magnetic susceptibility and is randomly distributed over the crystal volume. Random distribution of the "impurities" around the muon will produce Knight shift distribution with zero

average. However, when muon is localized near the "impurity", particular symmetry of this site with respect to the "impurity" provides large values of the dipolar Knight shift of certain (negative in our case) sign. Thus, the Knight shift distribution becomes shifted. But now we are faced with the problem of different temperature dependencies of the Knight shift broadening $k_\sigma(T)$ (which follows $\sigma(T)$ shown in fig. 12) and the $\chi(T)$ (fig. 1): while $k_\sigma(T)$ has a pronounced increase at temperatures below 80 K, $\chi(T)$ even slightly decrease in the same temperature interval. This puzzling feature can be understood if the coupling constant A_{eff} is temperature dependent, or if the coupling constant of muon with "impurity" is very large so that susceptibility of impurity affects the K_μ , but does not affect the bulk susceptibility, due to small "impurity" concentration.

6 Discussion and conclusions

In $\text{La}_2\text{CuO}_{4+y}$ the muon is not diffusing in the temperature interval under study $T < 130$ K. The exponential contribution to the muon spin relaxation found below 30 K, evidences that atomic spin fluctuations are slowing down. The fluctuation frequency of the electronic moments is decreased six times as the temperature is decreased from 30 K to 10 K. Assuming that the effective field at the muon is similar to those in stoichiometric antiferromagnetic La_2CuO_4 , where it is produced by Cu^{2+} ions we can estimate that the absolute value of spin fluctuation frequency at 10 K is $\nu_c \simeq 10^{10}$ Hz. To our opinion, the temperature 30 K, where we start to observe noticeable decrease of ν_c is not a critical point of this system. This just reflects the sensitivity of the experimental method. This process of the continuous slowing down of the electronic spin dynamics is probably extended from high temperatures, where fluctuations are too fast to be detected by μSR . Below the temperature $T_f = 8$ K very sharp decrease of the ν_c occurs, justifying on magnetic phase transition at this point. The muon spin relaxation rate increases two orders in magnitude, as the temperature decreases from 8 K to 3 K. The process of spin freezing develops in the part of crystal volume reaching the 1/2 fraction of the crystal at $T = 3$ K. The rest of the crystal remains in the paramagnetic state. According to X-ray and neutron diffraction data the crystal is in single phase and perfectly homogeneous. Typical scale of a crystallographic phase which certainly has to be detected by diffraction technique is less than 10^3 \AA . From the other hand the crystal reveals superconductivity - resistance becomes zero at $T_c = 12$ K. Presence of spin freezing below 8 K in a half of the sample volume allows to assume that phase separation into hole rich and hole poor regions still present, but on the microscopic scale of the order 10^2 \AA . Less scales (e.g 10 \AA) is hardly possible since the coherence length determined from dH_{c2}/dT data is $\xi \simeq 10 \text{ \AA}$. Intriguing question here is whether spin freezing develops in the whole crystal volume at further cooling below 3K. In this case superconductivity could be possibly suppressed at low temperatures. Additional evidence in favor of microscopical space separation of superconducting domains comes from the fact that in the TF experiment the muon spin relaxation rate does not have a sharp increase below the temperature of superconducting transition $T_c = 12$ K, which is usually observed due to formation of Abrikosov lattice. This implies that

superconducting domains in the crystal are too small in comparison with the London penetration depth, and can not keep even single vortex line.

TF μSR experiment have been carried out in the external field 2 kOe. Two main parameters being the results are: the muon Knight shift K_μ and the field induced broadening σ_b . Dipolar contribution to the K_μ has been calculated in assumption that the source of the dipolar magnetic fields is Cu^{2+} -ions, magnetized in accordance with the macroscopic magnetic susceptibility measured with the same crystal. This dipolar contribution and Lorentz fields cannot provide description of neither the absolute value of the K_μ nor its temperature dependence. The muon site used for dipolar calculations was chosen in the (ac) plane near apical oxygen. This site provides good correspondence with the ZF nuclear dipole data and ZF muon spin precession frequency [23] in AFM compositions of the La_2CuO_4 . To get the right values of the K_μ observed in present experiment one has to put the muon closer to the copper ions or assume another sources of the hyperfine field on the muon. Placing the muon closer to copper ion would contradict experimental ZF- μSR data. To get the agreement with the Knight shift data one has to assume that oxygen atoms possess an unpaired spins which produce significantly larger contribution the Knight shift because the muon is localized close to the oxygen ions.

Large field induced broadening σ_b of the field distribution on the muon has been observed in the single crystalline sample. σ_b scales with both external field and the Knight shift. Reduced broadening $k_\sigma = \sigma/\omega_{\text{ext}}$ is larger than 1000 ppm. It seems that such large broadening is specific feature of macroscopically non-PS $\text{La}_2\text{CuO}_{4+y}$. In TF μSR experiments with polycrystalline sample of $\text{La}_2\text{CuO}_{4+y}$, which demonstrates macroscopic PS [30], or with the $\text{La}_{2-x}\text{Sr}_x\text{CuO}_{4+y}$ [22, 28, 31] samples typical muon spin relaxation rate in paramagnetic state is $\sigma = 0.14 \mu\text{s}^{-1}$. It varies very slightly with the external field ($0.1 \text{ kOe} < H_{\text{ext}} < 4 \text{ kOe}$) implying that polycrystalline and any other broadening contributions are small. In our case of *single crystalline sample* the relaxation rate is significantly larger. For example, $\sigma \geq 0.3 \mu\text{s}^{-1}$ for external field 2 kOe for $H||c$, where nuclear dipole contribution amounts only $\sigma_n \simeq 0.2 \mu\text{s}^{-1}$. The muons have strongly different local magnetic environment in this macroscopically non-PS crystal. We has to assume that the crystal contains a magnetic "impurity" which is randomly distributed over the crystal. Rôle of "impurity" can belong to extra oxygen atoms in O^- state or atomic scale regions possessing large magnetic susceptibility.

The main result of the present work is the detection of electronic spin freezing in superconducting single crystal $\text{La}_2\text{CuO}_{4+y}$. We suggest that such a coexistence is realized in form of microscopic phase separation (PS). The $\text{La}_2\text{CuO}_{4+y}$ crystals with $y=0.03$ look homogeneous and single phase on the macroscopic level for neutron and X-ray diffraction and only the microprobe μSR -study allows to detect an inhomogeneity on the scale of 10^2 \AA . As to the origin of PS two reasons with different driving mechanism may be considered. First, because of the low oxygen mobility in the present crystals, one can end up in some kind of metastable system if approaching the thermodynamic equilibrium takes too long on the laboratory time-scale. In this case we can find ourselves at the very beginning of a decay process, possibly by spinodal mechanism without nuclear formation, when the concentration wave of composition extends over the whole crystal, producing a phase inhomogeneity on the micro-level. It means that

the system behaves like a phase separated one, but with very small particles of each phase below a temperature T_p , whereas in crystals with high oxygen diffusion usual (macroscopic) PS is observed. The second scenario for PS may be connected with pure electronic phase separation (EPS) driven by Coulomb forces when the system turns out to be unstable with respect to a separation onto regions with different hole concentrations. It should be pointed out that the EPS state, resembling to some extent the Wigner crystal, has a basically different ground state from the first scenario described above. If indeed the second possibility occurs, this would mean that the whole "T-y" phase diagram of $\text{La}_2\text{CuO}_{4+y}$ has to be revised.

7 Acknowledgments

This work was funded in part by Russian State Program on HTSC (project N93019)

References

- [1] V.J.Emery, S.A.Kivelson, H.Q.Lin, Phys. Rev. Lett. **64** (1990) 475. V.J.Emery, S.A.Kivelson, H.Q.Lin, Physica C **209** (1993) 597.
- [2] E.L.Nagaev, A.I.Podelshnikov, Zh. Eksp. Teor. Fiz. **104** (1993) 3643; E.L.Nagaev, Physica C **222** (1994) 324, and references herein.
- [3] E.Sigmund, V.Hizhnyakov, R.K. Kremer, A.Simon, Z. Phys. B **94** (1994) 17; R.K. Kremer, V.Hizhnyakov, E.Sigmund, A.Simon, K.A.Muller, Z. Phys. B **91** (1993) 169;
- [4] J.H.Cho, F.C.Chou, D.C.Johnston, Phys. Rev. Lett. **70** (1993) 222.
- [5] D.C.Johnston, F.Borsa, J.H.Cho, F.C.Chou, D.R.Torgeson, D.Vaknin, J.L.Zarestky, J.Ziolo, J.D.Jorgensen, P.G.Radaeli, A.J.Schultz, J.L.Wagner, S.-W.Cheong, JALCOM **207/208** (1994) 206.
- [6] A.Weidinger, Ch.Niedermayer, A.Golnik, R.Simon, E.Recknagel, J.I.Budnick, B.Chamberland, C.Baines Phys. Rev. Lett. **62** (1989) 102; H.Heffner, D.L.Cox, Phys. Rev. Lett. **63** (1989) 2538.
- [7] P.C.Hammel, A.P.Reyes, S.-W.Cheong, Z.Fisk, J.E.Schirber, Phys. Rev. Lett. **71** (1993) 440.
- [8] V.Chechersky, N.S.Kopelev, Beom-Hoan O, M.I. Larkin, J.L. Peng, J.T.Markert, R.L.Greene, A.Nath, Phys. Rev. Lett. **70** (1993) 3355.
- [9] J.Mesot, P.Allenspach, U.Staub, A.Furrer, H.Mutka, Phys. Rev. Lett. **70** (1993) 865.
- [10] Y.H. Kim, S.-W.Cheong, Z.Fisk, Physica C **200** (1992) 201..

- [11] S.Uchida, T.Ido, H.Takagi, T.Arima, Y.Tokura and S.Tajima, et al. , Phys. Rev. B **43** (1991) 7942.
- [12] J.D.Jorgensen, B.Dabrowski, S.Pei, D.G.Hinks, L.Soderholm, B.Morosin, J.E.Schirber, E.L.Venturini, D.S.Ginley, Phys. Rev. B **38** (1988) 11337; B.Dabrowski, J.D.Jorgensen, D.G.Hinks, S.Pei, D.R.Richards, H.B.Vanfleet, D.L.Decker, Physica C **162-164** (1989) 99.
- [13] P.G.Radaeli, J.D.Jorgensen, R.Kleb, B.A.Hunter, F.C.Chou, D.C.Johnston, Phys. Rev. B **49** (1994) 6239.
- [14] P.C.Hammel, et al. , Physica B **199-200** (1994) 235.
- [15] S.N.Barilo, A.P.Ges, S.A.Guretskii, D.I.Zhigunov, A.A.Ignatenko, I.D.Lomako, A.M.Luginets, V.N.Shambalev, et al. , Superconductivity **2** (1989) 156.
- [16] A.V.Bazhenov, K.B.Rezchikov, T.N.Fursova, A.A.Zakharov, M.B.Tsetlin, et al. , Physica C **214** (1993) 45.
- [17] A.A.Zakharov, M.B.Tsetlin, S.N.Barilo, P.V.Gritskov, Superconductivity **5** (1992) 207.
- [18] A.V.Bazhenov, A.V.Gorbunov, K.B.Rezchikov, T.N.Fursova, A.A.Zakharov, M.B.Tsetlin, et al. , Physica C **208** (1993) 197.
- [19] A.A.Zakharov, A.A.Nikonov, O.E.Parfionov, M.B.Tsetlin, V.M.Glaskov, N.V.Revina, S.N.Barilo, D.I.Zhigunov, L.A.Kurnevitch, Physica C **223** (1994) 157; A.A.Zakharov, S.N.Barilo, A.A.Nikonov, O.E.Parfionov, Physica C **235-240** (1994) 341.
- [20] A.N.Balagurov, V.Yu.Pomjakushin, V.G.Simkin, A.A.Zakharov, to be published.
- [21] A.A.Zakharov, A.A.Teplov, accepted in Superconductivity (1996).
- [22] V.G.Grebinnik, V.N.Duginov, V.A.Zhukov, S.Kapusta, A.B.Lazarev, V.G.Olshevsky, V.Yu.Pomjakushin, S.N.Shilov, I.I.Gurevich, B.F.Kirillov, B.A.Nikolsky, A.V.Pirogov, A.N.Ponomarev, V.A.Suetin I.P.Borovinskaya, M.D.Nersesyan, A.G.Peresada, Yu.F.Eltzev, V.R.Karasik, O.E.Omelyanovsky, Hyperfine Interactions **61** (1990) 1085.
- [23] B.Hitti, P.Birrer, K.Fischer, F.N.Gygax, E.Lippelt, H.Maletta, A.Schenck, M.Weber, Hyperfine Interactions **63** (1990) 287.
- [24] Y.J.Uemura, T.Yamazaki, D.R.Harshman, M.Senba, E.J.Ansaldo, Phys. Rev. B **31** (1985) 546.
- [25] I.A. Campbell et al. , Phys. Rev. Lett. **72** (1994) 1291.
- [26] Shukri B. Sulaiman, N.Sahoo, Sudha Srinivas, F.Hagelberg, T.P.Das Hyperfine Interactions **79** (1993) 901.

- [27] E.Torikai, H.Ishihara, K.Naganine, H.Kitazawa, I.Tanaka, H.Kojima, S.B.Sulaiman, S.Srinivas, T.P.Das *Hyperfine Interactions* **79** (1993) 915.
- [28] V.Yu.Pomjakushin, Doctoral thesis, JINR, Dubna, 1992.
- [29] K. Kumagai, Y.Nakamura *Physica C* **157** (1989) 307;
H. Lütgemeier, M.W.Pieper, *Solid State Commun.* **64** (1987) 267.
- [30] E.J.Ansaldo, J.H.Brewer, T.M.Riseman, J.E.Schirber, E.L.Vemturini, B.Morosin, D.S.Ginley, B.Sternlieb, *Phys. Rev. B* **40** (1989) 2555.
- [31] G.Aeppli, R.J.Cava, E.J.Ansaldo, J.H.Brewer, S.R.Kreitzman, G.M.Luke, D.R.Noakes, R.F.Kiefl, *Phys. Rev. B* **35** (1987) 7129.

Received by Publishing Department
on January 22, 1996.